

Optimizing the UE Transmission Probability for D2D Direct Discovery

David Griffith and Fiona Lyons
National Institute of Standards and Technology
Gaithersburg, Maryland 20899–6730
Email: david.griffith@nist.gov

Abstract—We model Mode 2 direct discovery in Device-to-Device (D2D) Long Term Evolution (LTE) networks and derive the optimal value of the discovery message transmission probability that minimizes the mean number of periods required for a successful discovery message transmission. We use Monte Carlo simulations to validate our analytical results and to show that optimizing the transmission probability produces nearly optimal performance with respect to the time required for all members of a group of User Equipments (UEs) to discover each other.

I. INTRODUCTION

As an enhancement of Long Term Evolution (LTE) systems beyond Release 12, Device-to-Device (D2D) communications allow User Equipments (UEs) to exchange data directly with other D2D-capable UEs, rather than by routing data from one UE over an uplink connection to a base station, which forwards the data over a downlink to the destination UE. The D2D connection from one UE to another UE, defined as a *sidelink* (SL) as an extension of the uplink/downlink (UL/DL) nomenclature, consists of a set of resources that can be used in Time Division Duplex (TDD) or Frequency Division Duplex (FDD) LTE deployments [1].

D2D was originally proposed as an underlay network that would offload intracell traffic from base stations while minimally interfering with intercell traffic, thus increasing network throughput by as much as 65 % [2], but the concept has since expanded. D2D-capable devices can support cell coverage extension by serving as relays for UEs that are outside the coverage area of any cellular base station [3]. Future D2D use cases include spectrum reuse, communication between UEs on opposite sides of the coverage boundary between two cells, and communication among UEs that are all outside any base station’s coverage area and which therefore must be capable of self-organization [4, Fig. 1]. The last scenario is of particular interest to the public safety community [5].

An important D2D function is *discovery*, the process by which D2D UEs identify themselves to each other, using a specific set of time and frequency resources contained in a Physical Sidelink Discovery Channel (PSDCH). UEs that

Disclaimer: Certain commercial software packages are identified in this paper in order to specify the experimental procedure adequately. Such identification is not intended to imply recommendation or endorsement by the National Institute of Standards and Technology, nor is it intended to imply that the software packages identified are necessarily the best available for the purpose.

transmit announcements over the PSDCH randomly choose resources from a shared pool when they are not in the coverage of a base station, which can happen in public safety deployment scenarios, for example. Since multiple UEs can choose a given resource simultaneously, collisions between discovery messages may prevent them from being received by other D2D UEs. To address this problem, UEs use a transmission probability to throttle their use of the PSDCH; however, if this parameter is set too low, it will needlessly hinder UEs from quickly disseminating discovery information. We therefore need to find the optimal value for the transmission probability.

In this paper, we develop a closed-form expression for the optimal transmission probability that depends on the resource pool size, the number of subframes in the pool, and the number of UEs that use the pool. We discuss prior work in this area in Section II; we describe the SL discovery process in Section III, and then develop the mathematical model. In Section IV, we validate the model and examine its sensitivity to variations in the input parameters. We use Monte Carlo simulations to show that the optimal transmission probability also approximately minimizes the mean number of transmission periods for every UE to receive a discovery message from every other UE, which further demonstrates its usefulness. In Section V, we summarize our results and discuss future work.

II. SURVEY OF PRIOR WORK

Several recent studies have addressed issues related to discovery transmission; we describe these and their relation to our work in the following. Park *et al.* developed a scheme to reduce what they call the “participation delay,” the time from a UE’s entry to the network to its first beacon transmission [6]. They define temporary discovery resources, which are a small subset of the discovery resource pool and are reserved for the exclusive use of newcomers to the network. They show that this approach reduces the participation delay for new arrivals while having little impact on UEs already in the network. It is possible to use our model to optimize the size of the temporary pool, which we are undertaking as part of our ongoing work.

Kang and Kang used a stochastic geometry approach to determine how many devices can be discovered in a given number of PSDCH periods [7], but their approach is substantially different from ours. They modeled the population of devices using a non-homogeneous Poisson Point Process

(PPP) and used the Signal to Interference and Noise Ratio (SINR) to determine whether a signal could be received by a UE that was a given distance from the transmitting UE, using a simple path loss model that incorporates fading. While they considered the effect of half-duplex devices, they did not model the transmission probability.

Finally, the work by Bagheri *et al.* uses a model that obtains the probability of a collision in a given discovery resource [8]. However, their analysis fails to account for the half-duplex effect. They also do not consider the probabilistic transmission mechanism. Baghari *et al.*, like Kang and Kang, examines the effect of the SINR on the collision rate, assuming uniformly distributed UEs. We do not consider the possibility of a high SINR's allowing reception of a discovery message in this paper; instead, we use the more conservative assumption that collisions result in the loss of all colliding messages. We are including SINR and channel effects in an expanded model.

III. THE MATHEMATICAL MODEL

A. The Sidelink Discovery Channel

Under Release 12, there are two D2D discovery modes for resource allocation [9, Clause 9.1.2]. Mode 1 discovery uses a base station to schedule and assign resources for transmitting discovery messages to UEs. With dedicated resources, UEs can operate without interference from other UEs that are associated with the same base station. In Mode 2, UEs autonomously choose resources from a pool; this reduces signaling but introduces the risk of collisions due to UEs' simultaneously randomly selecting the same resource. For out-of-coverage UEs, Mode 2 is the only possible option in the absence of a base station. The following analysis focuses on Mode 2 discovery.

The notation associated with the PSDCH and its attributes is listed in Table I. The PSDCH resource pool repeats periodically in the time domain; the period is given by the parameter P , which is set by the Information Element (IE) *discPeriod* [10, Clause 14.3.3]. The *discPeriod* IE is a parameter in the *SL-DiscResourcePool* IE, which is defined in [11, Clause 6.3.8].

Within each period, the PSDCH configuration variables *prb-Start*, *prb-End*, and *prb-Num*, which are respectively denoted by the variables $S1$, $S2$, and M , determine the range of subbands that the PSDCH occupies. The *SL-OffsetIndicator* IE gives the displacement of the pool from the first subframe in the period. The *SL-TF-ResourceConfig* IE [11, Clause 6.3.8] contains these IEs. A Physical Resource Block (PRB) with index m is part of the PSDCH if $S1 \leq m \leq S1 + M$ or $S2 - M \leq m \leq S2$. In the time domain, the set of subframes that compose the PSDCH is encoded in a bitmap defined by the IE *subframeBitmap*, where a bit that is set high indicates that the corresponding subframe is part of the PSDCH. The bitmap is repeated *numRepetition* times; this IE is located in the *SL-DiscResourcePool* IE [11, Clause 6.3.8]. In Fig. 1, we show the PSDCH structure and periodicity, and illustrate the role of the various PSDCH IEs.

A UE with a discovery message to send generates a uniformly distributed random value $p1 \in (0, 1]$. The UE sends

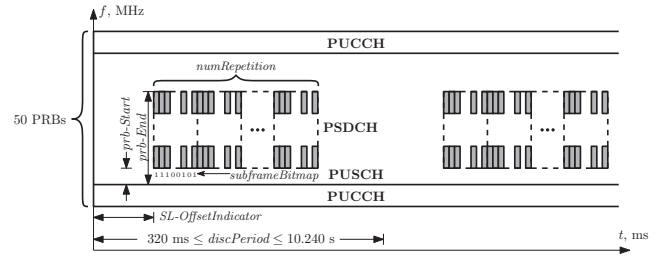


Fig. 1. The structure of the PSDCH resource pool.

its message if $p1$ is less than a threshold value *txProbability*, which is an IE within the *SL-DiscResourcePool* IE [12, Clause 5.15.1.1]. The *txProbability* IE can take one of the following four values: p25, p50, p75, and p100; these values denote thresholds of 0.25, 0.50, 0.75, and 1.00 respectively.

UEs transmit discovery messages using pairs of PRBs in the PSDCH¹. A transport block occupies two PRBs per slot in a single subframe [10, Clause 14.3.1]. The network operator can select the number of times each transport block is transmitted, $1 \leq N_{SLD}^{TX} \leq 4$. For Mode 2 SL discovery, the PRBs of the j th transmission in the i th PSDCH period are in subframe $l_{N_{SLD}^{TX} b_j^{(i)} + j - 1}^{PSDCH}$ and occupy the PRB indices $m_{2a_j^{(i)}}^{PSDCH}$ and $m_{2a_j^{(i)} + 1}^{PSDCH}$, where

$$a_j^{(i)} = ((j - 1) \lfloor N_f / N_{SLD}^{TX} \rfloor + \lfloor n_{PSDCH} / N_t \rfloor) \bmod N_f \quad (1a)$$

$$b_j^{(i)} = n_{PSDCH} \bmod N_t. \quad (1b)$$

In Eq. (1), $N_f = \lfloor M_{RB}^{PSDCH_RP} / 2 \rfloor$ is the number of PRB pairs in the frequency domain, where $M_{RB}^{PSDCH_RP}$ is the number of PRBs in the PSDCH, $N_t = \lfloor L_{PSDCH} / N_{SLD}^{TX} \rfloor$ is the number of subframe sets in the time domain, where L_{PSDCH} is the number of subframes spanned by the PSDCH, and n_{PSDCH} is the resource index. The sender chooses n_{PSDCH} randomly from the set of $N_r = N_f N_t$ integers $\{0, 1, \dots, N_r - 1\}$ [12, Clause 5.15.1.1]. If two UEs choose the same value of n_{PSDCH} , all N_{SLD}^{TX} of their transmissions will collide.

In Fig. 2, we show the placements of groups of PRB pairs for a hypothetical PSDCH consisting of $M_{RB}^{PSDCH_RP} = 8$ PRBs in the frequency domain and $L_{PSDCH} = 12$ subframes in the time domain for $N_{SLD}^{TX} = 2$ and $N_{SLD}^{TX} = 4$ transmissions. Eq. (1) assigns resources to a set of transmissions such that the N_{SLD}^{TX} transmissions occur over a sequential series of subframe indices, and also over a sequential series of PRB pair indices, modulo N_f . Most importantly, the set of resource index values associated with a given subframe index i is identical to the set of resource index values in subframes $i + 1, i + 2, \dots, i + N_{SLD}^{TX} - 1$. Thus, half-duplex UEs that choose values of n_{PSDCH} that produce identical values of $b_j^{(i)}$ will be unable to receive any of one another's transmissions for all values of j in a given PSDCH period, i . Because values of n_{PSDCH} that produce identical subframe

¹A PRB spans twelve 15 kHz subcarriers and occupies a slot that is half of a 1 ms subframe.

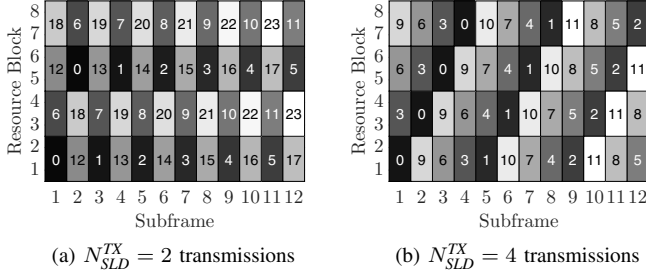


Fig. 2. Resources in PSDCH resource pool with $M_{RB}^{PSDCH,RP} = 8$ PRBs and $L_{PSDCH} = 12$ subframes, from Eqs. (1a) and (1b).

TABLE I
LIST OF SYMBOLS

Symbol	Definition
$\mathcal{N}(A)$	Number of occurrences of event A
$\Pr\{A\}$	Probability that event A occurs
$E\{Z\}$	Expected value of random variable Z
L_{PSDCH}	Number of subframes spanned by the PSDCH
$M_{RB}^{PSDCH,RP}$	Number of PRBs occupied by the PSDCH
N_{SLD}^{TX}	Number of SL discovery transport block transmissions
l_{PSDCH}^i	i th subframe in the PSDCH, $0 \leq i < L_{PSDCH}$
m_j^{PSDCH}	j th PRB slot in the PSDCH, $0 \leq j < M_{RB}^{PSDCH,RP}$
N_f	Number of PRB pairs in discovery pool
N_t	Number of subframe sets in discovery pool
N_r	Number of resources in discovery pool, $N_r = N_f N_t$
n_{PSDCH}	Discovery resource index
P	PSDCH period duration
θ	UE transmission probability
θ^*, θ_q^*	Optimal and quantized optimal values of θ
\mathcal{G}	The set of UEs in a D2D group of interest
N_u	Number of UEs in D2D group \mathcal{G}
X, Y	Randomly chosen UEs from D2D group \mathcal{G}
δ_X	Discovery message sent by UE X from D2D group \mathcal{G}
S_X	Set of subframes occupied by δ_X
$N_{Y \rightarrow X}$	Number of PSDCH periods for UE X to discover UE Y
$N_{G \rightarrow \mathcal{G}}$	Number of PSDCH periods for discovery of all UEs in \mathcal{G}
$P_{Y \rightarrow X}(\theta)$	$\Pr\{\text{UE } X \text{ receives UE } Y\text{'s message in a given period}\}$
$\hat{P}_{N_{Y \rightarrow X}}(\theta)$	Estimated value of $P_{Y \rightarrow X}(\theta)$
$\hat{\sigma}_{\hat{P}_{N_{Y \rightarrow X}}(\theta)}^2$	Sample variance of $\hat{P}_{N_{Y \rightarrow X}}(\theta)$
$\Delta\mu_{Y \rightarrow X}$	Change in $E\{N_{Y \rightarrow X}(\theta^*)\}$ due to quantizing θ
n	Index indicating the n th PSDCH period

assignments for a given transmission attempt produce identical subframe assignments for all other transmission attempts in the same PSDCH period. Thus, we can treat all N_{SLD}^{TX} subframes associated with a particular value of n_{PSDCH} as a single entity.

B. Model Description

We model the Discovery Resource Pool as a matrix with N_f rows and N_t columns that consists of $N_r = N_f N_t$ resources as shown in Fig. 3. Each row corresponds to a PRB pair, while each column corresponds to a subframe set. There are N_u UEs in group \mathcal{G} that use the resource pool. Each UE transmits a discovery message during each period by choosing

a resource in the pool with uniform probability. We assume that UEs choose resources independently of each other.

The \times 's in the boxes in Fig. 3 show the presence of discovery messages; the number of \times 's indicates the number of discovery messages. We assume that if more than one discovery message occupies a resource, then all of the co-located messages will be lost due to mutual interference. The \otimes symbol indicates δ_X , the discovery message generated by UE X , and the column containing δ_X , which corresponds to S_X , is highlighted. Let S_X be the set of subframes occupied by UE X 's discovery message. A half-duplex UE cannot transmit and receive at the same time, and thus misses any discovery messages that other UEs send in the subframes in which it is transmitting. Thus any discovery messages transmitted in S_X by other UEs in \mathcal{G} will not be received by UE X .

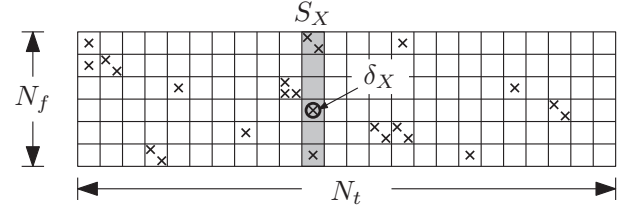


Fig. 3. A resource pool with $N_r = N_f N_t$ discrete resources organized into N_f frequency slots and N_t subframe sets, where S_X , the set of subframes used by UE X to transmit its discovery message, δ_X , is highlighted.

Let X and Y be two UEs chosen randomly from \mathcal{G} . Let $\{Y \rightarrow X\}$ be the event, "UE X successfully receives discovery message δ_Y from UE Y ," and let $\{\delta_Y \in S_X\}$ be the event, "UE Y sends discovery message δ_Y in subframe S_X ." A UE uses the same value of the parameter $p1$ to determine whether to transmit all N_{SLD}^{TX} of its transmission attempts in a PSDCH period. Thus, we can treat all of a period's transmissions by a UE as a single event and apply the resource grid that we introduced in Fig. 3.

Let $\theta = \Pr\{p1 \leq txProbability\} = \Pr\{Y \text{ transmits}\}$. We define $P_{Y \rightarrow X}(\theta)$ in Table I; and it follows that $P_{Y \rightarrow X}(\theta) = \theta \Pr\{Y \rightarrow X | Y \text{ transmits}\}$. By Bayes' Theorem,

$$\Pr\{Y \rightarrow X | Y \text{ transmits}\} = \Pr\{Y \rightarrow X | \delta_Y \in S_X\} \Pr\{\delta_Y \in S_X\} + \Pr\{Y \rightarrow X | \delta_Y \notin S_X\} \Pr\{\delta_Y \notin S_X\}. \quad (2)$$

In this case, the event $\{\delta_Y \in S_X\}$ occurs when UE X transmits (independently of all other UEs in the group, with probability θ) and UE Y 's message δ_Y falls within the subframe set S_X . It follows that $\Pr\{\delta_Y \in S_X\} = \theta/N_t$, since UE X 's decision to transmit and UE Y 's choice of a subframe set are independent. As before, $\Pr\{Y \rightarrow X | \delta_Y \in S_X\} = 0$ since UE X and UE Y will not receive each others' message if they transmit in the same subframes. To determine $\Pr\{Y \rightarrow X | \delta_Y \notin S_X\}$, we condition on how many of the remaining $(N_u - 2)$ UEs transmit, which has a binomial distribution with probability mass function $f(k; N_u - 2, \theta) = \binom{N_u - 2}{k} \theta^k (1 - \theta)^{(N_u - 2) - k}$. The probability a

UE that transmits does not use UE Y 's resource is $(1 - 1/N_r)$. Thus Eq. (2) becomes

$$\Pr\{Y \rightarrow X \mid Y \text{ transmits}\} = 0 \cdot \frac{\theta}{N_t} + \left(1 - \frac{\theta}{N_t}\right) \sum_{k=0}^{N_u-2} \left(1 - \frac{1}{N_r}\right)^k f(k; N_u - 2, \theta). \quad (3)$$

We recall that $P_{Y \rightarrow X}(\theta) = \theta \Pr\{Y \rightarrow X \mid Y \text{ transmits}\}$; we simplify Eq. (3) and apply the Binomial Theorem, and get

$$P_{Y \rightarrow X}(\theta) = \theta \left(1 - \frac{\theta}{N_t}\right) \left(1 - \frac{\theta}{N_r}\right)^{N_u-2}. \quad (4)$$

Assuming that the resource selection processes in different periods are independent, it follows that the number of periods for UE X to discover UE Y , $N_{Y \rightarrow X}(\theta)$, has a geometric distribution. Thus, the mean number of periods for UE X to discover UE Y is $E\{N_{Y \rightarrow X}(\theta)\} = 1/P_{Y \rightarrow X}(\theta)$.

C. Optimizing the Transmission Probability

We can determine the value of θ that maximizes $P_{Y \rightarrow X}(\theta)$ by differentiating Eq. (4):

$$\frac{dP_{Y \rightarrow X}(\theta)}{d\theta} = \frac{(N_r - \theta)^{N_u-3} [N_r(N_t - 2\theta) + \theta(N_t - N_t N_u + \theta N_u)]}{N_r^{N_u-2} N_t}. \quad (5)$$

The derivative is zero when $\theta = N_r$, but this is not a valid solution. The polynomial in θ within the square brackets in the numerator of Eq. (5), $N_r \theta^2 - (2N_r - N_t + N_t N_u)\theta + N_r N_t$, is zero when

$$\theta = \frac{2N_r + N_t(N_u - 1) \pm \sqrt{4N_r(N_r - N_t) + N_t^2(N_u - 1)^2}}{2N_u}. \quad (6)$$

Because $N_t \leq N_r$, the expression under the radical is always non-negative. Additionally, the positive branch is greater than or equal to unity². Thus the negative branch of Eq. (6) gives θ^* , the optimal value of θ . We use the second derivative to verify that θ^* maximizes $P_{Y \rightarrow X}(\theta)$ as follows:

$$\ddot{P}_{Y \rightarrow X}(\theta^*) \stackrel{\text{def}}{=} \left. \frac{d^2 P_{Y \rightarrow X}(\theta)}{d\theta^2} \right|_{\theta=\theta^*} = \frac{-A}{N_r N_t} \left(\frac{A+B}{2N_r N_u} \right)^{N_u-3}, \quad (7)$$

where $A = \sqrt{4N_r(N_r - N_t) + N_t^2(N_u - 1)^2}$ and $B = (2N_r - N_t)(N_u - 1)$. Since $N_t \leq N_r$, it follows that $A > 0$ and $B > 0$; thus, $\ddot{P}_{Y \rightarrow X}(\theta^*) < 0$ and $P_{Y \rightarrow X}(\theta^*)$ is a local maximum.

Depending on the relative values of the parameters N_r , N_t , and N_u , θ^* may fall outside the unit interval, i.e., $[0, 1]$. Expanding and simplifying the expression $\theta > 1$ using the negative branch of θ in Eq. (6) gives

$$N_u < \frac{N_r(N_t - 2) + N_t}{N_t - 1}. \quad (8)$$

²When $N_r = N_t = 1$, $\theta = 1$; and, the numerator of θ is greater than $2N_u$ when $1 < N_t \leq N_r$.

Thus, θ^* should be set to unity when the number of UEs is sufficiently small for Eq. (8) to hold.

IV. NUMERICAL RESULTS

A. Model Validation

We validated this model by running Monte Carlo simulations to estimate $P_{Y \rightarrow X}(\theta)$. The simulation consisted of a set of runs; each run in turn was composed of a set of individual trials. Each trial simulated the UE group's resource selections over a series of PSDCH periods, using a given value of θ for all UEs in the group. In each period, the simulator generated a $N_f \times N_t$ matrix that represented the PSDCH resource pool, and randomly placed UE Discovery messages in the matrix.

The simulator determines whether a successful transmission from UE Y to UE X has occurred by examining the placement of UE X 's transmission in relation to all other UEs. If UE X transmits in the same subframe set as UE Y , then UE X cannot receive UE Y 's discovery message. If any of the other $(N_u - 2)$ UEs transmits in the resource block chosen by UE Y , then the transmissions collide and UE Y 's message fails to reach UE X . The simulator also models the transmission probability θ , which is the same for all UEs, by having each UE generate a uniform random variate $0 < p_1 \leq 1$; if $p_1 \leq \theta$, then the UE chooses a resource for transmission. Thus UE Y 's transmission fails if UE Y generates a variate that is greater than θ . Also note that if the variate that UE X generates is not less than θ , the transmission succeeds as long as no other UE's message occupies the resource chosen by UE Y .

The simulator repeated this process until the occurrence of a successful transmission, at which time it recorded $N_{Y \rightarrow X}(j)$, the number of PSDCH periods required to achieve the success in the j th trial, and started a new trial if there were trials remaining in the run. Using the set of trial results $\{N_{Y \rightarrow X}(j)\}_{j=1}^{N_{\text{trials}}}$, the estimate for $P_{Y \rightarrow X}(\theta)$ from the i th run is

$$\hat{P}_{Y \rightarrow X,i}(\theta) = \frac{\mathcal{N}(N_{Y \rightarrow X}(\theta) = n)}{N_{\text{trials}}}, \quad (9)$$

where $\mathcal{N}(A)$ is the occurrence count of event A and N_{trials} is the number of trials per run. The estimated probability is

$$\hat{P}_{Y \rightarrow X}(\theta) = \frac{\sum_{i=1}^{N_{\text{runs}}} \hat{P}_{Y \rightarrow X,i}(\theta)}{N_{\text{runs}}} = \frac{\sum_{i=1}^{N_{\text{runs}}} \mathcal{N}(N_{Y \rightarrow X}(\theta) = n)}{N_{\text{runs}} N_{\text{trials}}} \quad (10)$$

and the estimator of the variance of $\hat{P}_{Y \rightarrow X}(\theta)$ is

$$\hat{\sigma}_{\hat{P}_{Y \rightarrow X}(\theta)}^2 = \frac{1}{N_{\text{runs}} - 1} \sum_{i=1}^{N_{\text{runs}}} \left(\hat{P}_{Y \rightarrow X,i}(\theta) - \hat{P}_{Y \rightarrow X}(\theta) \right)^2. \quad (11)$$

The simulation used 10 runs, with 50 trials per run. The resource pool contained $N_r = 50$ resources, with $N_f = 10$ PRB pairs and $N_t = 5$ subframe sets. In Fig. 4, we plot both the theoretical values of $P_{Y \rightarrow X}(\theta)$ and the Monte Carlo estimates with 95 % confidence intervals for $N_u \in \{5, 10, \dots, 50\}$ UEs³. We used the four enumerated values

³In some scenarios, the UE population may be larger, but this analysis can be readily extended to greater values of N_u and shows similar agreement between theoretical and simulation results.

for $txProbability$ for our θ values. The plots show good agreement between the theoretical and Monte Carlo results. Also, applying Eq. (8) indicates that we should set $\theta^* = 1$ when $N_u < 38.75$ UEs; the curves in the figure agree with this result. We examined other values of N_f and N_t and found similar agreement between the theoretical and Monte Carlo values; we do not show these plots due to space limitations.

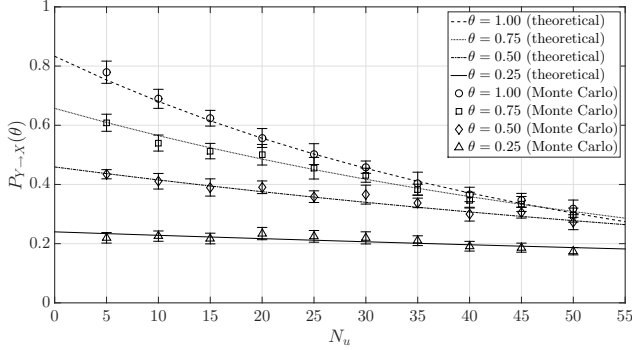


Fig. 4. Theoretical and simulated values of $P_{Y \rightarrow X}(\theta)$ plotted versus N_u , where $\theta \in \{0.25, 0.50, 0.75, 1.00\}$, for $N_f = 10$ PRB pairs and $N_t = 5$ subframe sets, with 95 % confidence intervals shown.

B. Sensitivity analysis

Next, we examine the effect of varying input parameters on the mean time to receive a discovery message. In Fig. 5, we show plots for two resource pool configurations, and examine the effect of varying N_r , N_t , and N_u . The greatest impact is due to reductions in N_r or N_t . $E\{N_{Y \rightarrow X}(\theta^*)\}$ varies roughly linearly with respect to the percentage change in N_u .

We are especially interested in the impact of variations in N_u when θ^* has been chosen based on a particular value for the group size. In Fig. 6, we plot $E\{N_{Y \rightarrow X}(\theta^*)\}$ versus N_u as a discrete sequence of points⁴. Next, for each value of N_u , we modify N_u by a fixed percentage, while keeping θ^* fixed, and recompute $E\{N_{Y \rightarrow X}(\theta)\}$ using the new value of N_u . We plot the resulting sets of values for $\pm 10\%$ and $\pm 50\%$ variations in N_u in the figure; we show the envelopes traced by the modified values rather than discrete points for the sake of clarity.

The figure shows that $E\{N_{Y \rightarrow X}(\theta^*)\}$'s sensitivity to variations in N_u increases as N_u itself increases, with a discontinuity in the slope of each envelope curve visible at $N_u = 38.75$ UEs, the threshold value given by Eq. (8). A $\pm 10\%$ deviation in N_u results in a variation of about half of a period when $N_u = 60$ UEs, and a variation of about one period when $N_u = 100$ UEs. When the variation is very large ($\pm 50\%$), increases in N_u have more effect than decreases.

Next we consider the impact of quantizing θ . In Section III we noted that θ can take only values that are multiples of $1/4$. Let $\theta_q^* = \max(1/4, \lceil 4(\theta^* - 1/8) \rceil / 4)$ be the value of θ^* rounded to the closest allowed value of $txProbability$. In Fig. 7, we plot $\Delta\mu_{Y \rightarrow X} \stackrel{\text{def}}{=} E\{N_{Y \rightarrow X}(\theta_q^*)\} - E\{N_{Y \rightarrow X}(\theta^*)\}$

⁴We chose $E\{N_{Y \rightarrow X}(\theta^*)\}$ rather than its reciprocal, $P_{Y \rightarrow X}(\theta^*)$, because the effects of variations in N_u are easier to see in the plot.

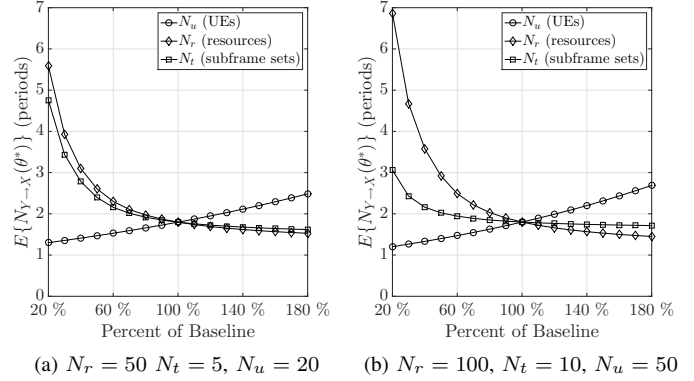


Fig. 5. Spider plots for two example PSDCH configurations.

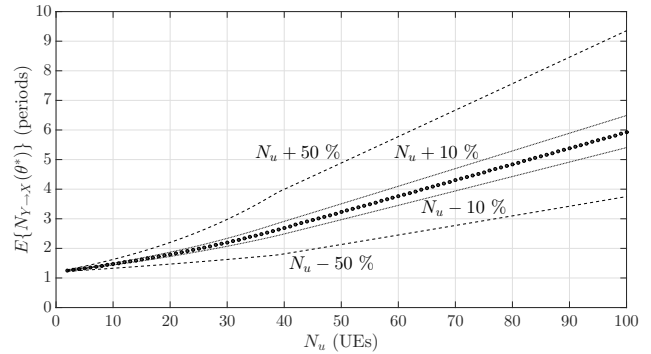


Fig. 6. Sensitivity plot of $E\{N_{Y \rightarrow X}(\theta^*)\}$ versus N_u for $N_f = 10$ PRB pairs and $N_t = 5$ subframe sets, showing the effect of 10 % and 50 % errors in the value of N_u .

versus N_u , using the same resource pool dimensions as before. Since θ_q^* is suboptimal, $E\{N_{Y \rightarrow X}(\theta_q^*)\} \geq E\{N_{Y \rightarrow X}(\theta^*)\}$. Note that $\theta^* = 0.25, 0.5, 0.75$ when $N_u = 191, 90, 56$ UEs, respectively, and that $\theta^* = 1$ for $N_u < 39$ UEs; at these values of N_u , $\Delta\mu_{Y \rightarrow X} \approx 0$ periods. The discontinuities in Fig. 7 are products of the step discontinuities in the mapping that produces θ_q^* (e.g., $\theta_q^* = \frac{1}{2}$ for $70 \text{ UEs} \leq N_u \leq 123 \text{ UEs}$ but $\theta_q^* = \frac{1}{4}$ for $N_u \geq 124 \text{ UEs}$). The figure shows that quantization introduces a penalty of at most half a period for most values of N_u ; the penalty increases to a period only as N_u approaches 275 UEs. We examined other pool configurations and observed similar behavior; a rule of thumb appears to be that $\Delta\mu_{Y \rightarrow X} > 1$ period if $N_u \gtrsim 5N_r$.

C. Impact of θ^* on group discovery time

Finally, we use Monte Carlo simulations to determine whether $\theta = \theta^*$ optimizes other performance metrics, particularly $E\{N_{\mathcal{G} \rightarrow \mathcal{G}}(\theta)\}$, the mean number of periods for every UE in \mathcal{G} to discover every other UE in \mathcal{G} . Each Monte Carlo trial used a $N_u \times N_u$ connectivity matrix to track the discovery status of each UE in \mathcal{G} . In each period, each UE chose a resource randomly, the ability of each UE to detect other UEs' messages was checked, and the connectivity matrix was updated. From these results we produced $\hat{E}\{N_{\mathcal{G} \rightarrow \mathcal{G}}(\theta)\}$.

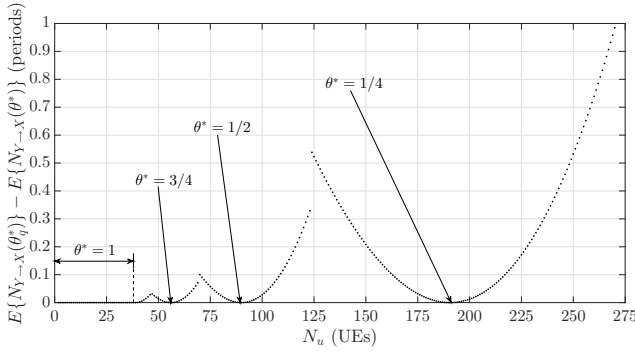
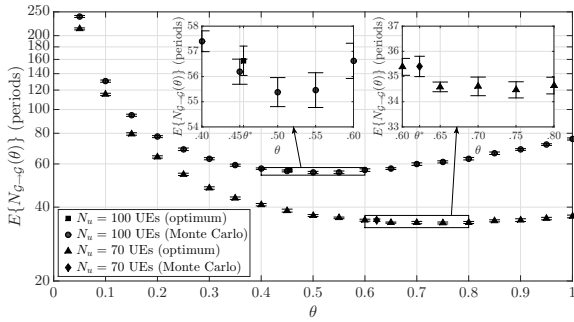
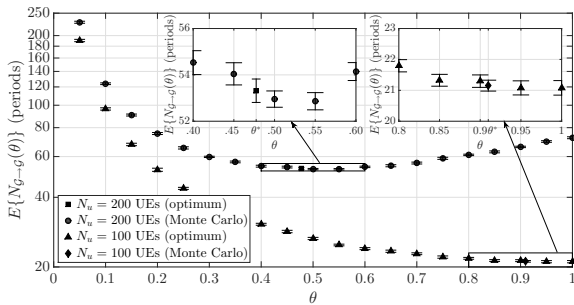


Fig. 7. Plot of $E\{N_{Y \rightarrow X}(\theta^*)\} - E\{N_{Y \rightarrow X}(\theta^*)\}$ versus N_u for $N_f = 10$ PRB pairs and $N_t = 5$ subframe sets, showing the effect of the quantization of θ .

Fig. 8, shows simulation results for two pool sizes, with $N_u = 100$ UEs and $N_u = 200$ UEs. We used 20 runs of 50 trials each to plot $\hat{E}\{N_{G \rightarrow G}(\theta^*)\}$ vs. θ , with 95 % confidence intervals. In each case, θ^* is close to the value of θ that minimizes $E\{N_{G \rightarrow G}(\theta)\}$. Regarding the quantization of θ , θ_q^* tends to give the best possible discovery performance for the whole group, although there are exceptions such as the case $N_u = 70$ UEs as shown in Fig. 8a; in this case, the quantization gives $\theta_q^* = 0.5$, although $\theta_q^* = 0.75$ is the better choice. Our simulations have shown that θ^* tends to be less than the value of θ that optimizes group discovery performance, so rounding up to the next higher multiple of $1/4$ may give consistently near-optimal performance.



(a) $N_f = 10$ PRB pairs and $N_t = 5$ subframe sets



(b) $N_f = 10$ PRB pairs and $N_t = 10$ subframe sets

Fig. 8. $\hat{E}\{N_{G \rightarrow G}(\theta)\}$ versus θ , with 95 % confidence intervals shown.

V. SUMMARY AND FUTURE WORK

In this paper, we derived the optimal value for the UE transmission probability while accounting for the half-duplex nature of UE transmissions. We used this model to derive the maximum UE group size for which the optimal value of $txProbability$ is unity. We validated this model and showed that there is a small impact to performance when quantizing θ^* to multiples of $1/4$, as allowed by the 3GPP standard. We demonstrated that θ^* appears to closely track the value of θ that minimizes the mean number of periods for all UEs in a group to discover each other, although this result needs further confirmation. Our next steps include accounting for channel effects in the model, and examining the effect of synchronization errors on PSDCH performance.

REFERENCES

- [1] D. Astely, E. Dahlman, G. Fodor, S. Parkvall, and J. Sachs, "LTE release 12 and beyond [accepted from open call]," *IEEE Commun. Mag.*, vol. 51, no. 7, pp. 154–160, July 2013.
- [2] K. Doppler, M. Rinne, C. Wijting, C. Ribeiro, and K. Hugl, "Device-to-device communication as an underlay to LTE-advanced networks," *IEEE Commun. Mag.*, vol. 47, no. 12, pp. 42–49, December 2009.
- [3] X. Ma, R. Yin, G. Yu, and Z. Zhang, "A distributed relay selection method for relay assisted Device-to-Device communication system," in *IEEE 23rd Int. Symp. Personal Indoor and Mobile Radio Communications (PIMRC)*, September 2012, pp. 1020–1024.
- [4] X. Lin, J. Andrews, A. Ghosh, and R. Ratasuk, "An overview of 3GPP device-to-device proximity services," *IEEE Commun. Mag.*, vol. 52, no. 4, pp. 40–48, April 2014.
- [5] T. Doumi, M. Dolan, S. Tatesh, A. Casati, G. Tsirtsis, K. Anchan, and D. Flore, "LTE for public safety networks," *IEEE Commun. Mag.*, vol. 51, no. 2, pp. 106–112, February 2013.
- [6] S. Park and S. Choi, "Expediting D2D discovery by using temporary discovery resource," in *2014 IEEE Global Communications Conf. (GLOBECOM)*, December 2014, pp. 4839–4844.
- [7] H. Kang and C. Kang, "Performance analysis of device-to-device discovery with stochastic geometry in non-homogeneous environment," in *2014 Int. Conf. Information and Communication Technology Convergence (ICTC)*, October 2014, pp. 407–412.
- [8] H. Bagheri, P. Sartori, V. Desai, B. Classon, M. Al-Shalash, and A. Soong, "Device-to-device proximity discovery for LTE systems," in *2015 IEEE Int. Conf. Communication Workshop (ICCW)*, June 2015, pp. 591–595.
- [9] 3GPP, "Study on LTE Device to Device Proximity Services; Radio Aspects," 3rd Generation Partnership Project (3GPP), TR 36.843 V12.0.1, March 2014. [Online]. Available: http://www.3gpp.org/ftp/Specs/archive/36_series/36.843/36843-c01.zip
- [10] —, "Evolved Universal Terrestrial Radio Access (E-UTRA); Physical layer procedures," 3rd Generation Partnership Project (3GPP), TS 36.213 V12.7.0, September 2015. [Online]. Available: http://www.3gpp.org/ftp/Specs/archive/36_series/36.213/36213-c70.zip
- [11] —, "Evolved Universal Terrestrial Radio Access (E-UTRA); Radio Resource Control (RRC); Protocol specification," 3rd Generation Partnership Project (3GPP), TS 36.331 V12.7.0, September 2015. [Online]. Available: http://www.3gpp.org/ftp/Specs/archive/36_series/36.331/36331-c70.zip
- [12] —, "Evolved Universal Terrestrial Radio Access (E-UTRA); Medium Access Control (MAC) protocol specification," 3rd Generation Partnership Project (3GPP), TS 36.321 V12.7.0, September 2015. [Online]. Available: http://www.3gpp.org/ftp/Specs/archive/36_series/36.321/36321-c70.zip